Thermal decay in the one-dimensional transient thermal grating experiment using modified Debye-Callaway model

Younès Ezzahri *

Institut Pprime, CNRS, Université de Poitiers, F-86962 Futuroscope Chasseneuil, France

(Received 5 January 2022; revised 12 July 2022; accepted 30 August 2022; published 13 September 2022)

We calculate the thermal decay in the one-dimensional transient thermal grating (TTG) experiment by solving the transient Boltzmann-Peierls transport equation (BPTE) within the framework of the single-mode relaxation time approximation and using modified Debye-Callaway model in which both longitudinal and transverse phonon modes are included explicitly. We consider surface heating of an opaque thick semiconductor (SC) crystal film that we assume to have a cubic symmetry and is treated as a continuum, elastic, isotropic, and dispersionless medium. We obtain a nonuniversal spectral suppression function (SSF) in the integrand of the effective apparent thermal conductivity that is similar to the one obtained by Chiloyan *et al.* [Phys. Rev. B **93**, 155201 (2016)] using the standard single-mode relaxation time approximation (RTA) model. Therefore, the nonuniversal character of the SSF in the TTG experiment does not depend on the form of the collision operator approximation in the BPTE: Callaway's or standard. Moreover, the analysis of the behavior of the thermal decay rate shows how the peculiar crystal momentum shuffling effect of phonon-phonon scattering Normal processes (N processes) that is captured by Callaway's model influences the onset of the nondiffusive (quasiballistic) regime in the phonon transport process in SC crystals. This effect tends independently from the other phonon scattering processes to favor the maintenance of the phonon diffusive regime over a large length-scale range, a remarkable feature that cannot be put into light with the standard RTA model used in previous works. Hence, the implicit effect of N processes has certainly an important impact on the extraction of the phonon mean-free path spectrum distribution, especially in the high-temperature regime.

DOI: 10.1103/PhysRevB.106.125203

I. INTRODUCTION

For the purpose of heat transport in semiconductor (SC) and dielectric materials, the most important characteristic intrinsic length is the mean-free path (MFP) of phonons that represent the main energy (heat) carriers in these materials [1–4].

Transient thermal grating (TTG) spectroscopy technique has been proven to be a robust method to study length-scale based quasiballistic (nondiffusive) phonon transport, including the transition from the quasiballistic regime to the diffusive regime, in dielectric and SC crystals [5–9]. Using a reconstruction method, the TTG spectroscopy technique has allowed probing the phonon MFP spectrum distribution and obtaining valuable information about the contribution weight and role of low- and high-frequency phonons in the heat transport process in these materials [5].

In this technique, two crossed laser pulses are shone on the surface of a thin or thick film material. The film can be either suspended or deposited on a supporting substrate. The interference pattern of the pulses results in a spatially sinusoidal temperature profile that constitutes the thermal grating with a spatial period that can be varied by adjusting the angle between the crossed laser beams. Once heated, the sample is allowed to relax and the timely decay of the thermal profile is measured to yield information about the in-plane phonon transport process within the material [5–9]. Because of the great importance TTG has gained in the study of phonon spectroscopy, its modeling has become critical. So far, three approaches have been suggested to mathematically model the TTG technique in a one-dimensional case. (i) The first approach was performed in the framework of a "two-fluid" model by Maznev *et al.* [10]. An analytical spectral suppression function (SSF) in the integrand of the effective apparent thermal conductivity was obtained using simplifying assumptions about the scattering of high- and low-frequency phonons. This SSF was later utilized in the reconstruction of the phonon MFP spectrum distribution by Minnich [5]. As mentioned by Hua and Minnich [11] and Chiloyan *et al.* [12], there is a concern as the extent of validity of the two-fluid model is not clear. (ii) The second approach is based on solving the transient Boltzmann-Peierls transport equation (BPTE) in the framework of the standard single-mode relaxation time approximation (RTA) model. In the standard RTA model, all phonon-phonon scattering processes are treated similarly regarding the onset of thermal conduction, with no distinction whatsoever between Normal and Umklapp anharmonic processes [11,13]. This second approach was first explored by Collins *et al.*, where they used analytical and numerical methods to solve the problem and obtained the exact solution of the BPTE, in both the gray case and the full spectral case for Si and PbSe [13]. The authors showed that there is a deviation of the two-fluid model

* younes.ezzahri@univ-poitiers.fr

from the exact numerical solution for PbSe [13]. Hua and Minnich extended this same second approach to obtain the Fourier transform with respect to time of the thermal decay analytically. The authors were able to recover the two-fluid model SSF in what they called the "weakly quasi-ballistic regime" [11]. (iii) The third approach is a variational one that was first used by Chiloyan *et al.* to solve the transient BPTE using also the standard RTA model [12]. The authors found a different SSF than the one obtained earlier [10,11,13]. The authors argued afterwards about the nonuniversality of the SSF, as the one they obtained depends explicitly on the material properties. The SSF obtained by Maznev *et al.* [10], Collins *et al.* [13], and Hua and Minnich [11] is a universal one; i.e., it depends only on the ratio of the phonon MFP with respect to a characteristic length and not otherwise on the material properties. A more detailed and extended analysis of the application of the variational approach to include the effect of the two-dimensional case of phonon transport in a TTG configuration was later presented by Chiloyan *et al.* [14] and Hubermann *et al.* [15]. The authors showed that the optical penetration depth could have an important effect for thin-film materials that are transparent or semitransparent to the laser wavelength used in the TTG experiment [14,15].

Two recent works by Hua and Lindsay [16] and Chiloyan *et al.* [17] went beyond the standard RTA model and applied a more elaborate method using the full linearized collision matrix. The authors obtained closed-form expressions for the temperature profile and the effective apparent thermal conductivity and highlighted the limits of the standard RTA model in treating the results of the TTG spectroscopy technique, especially for high thermal conductivity materials.

The differences in the outcomes of all these approaches show clearly how critical and crucial the modeling of the TTG spectroscopy technique is, for a better and rigorous understanding of phonon transport regimes in this experimental configuration. Besides, no analysis so far has considered Callaway's model or a detailed analysis of the effect of temperature.

The motivation behind the present work is to calculate and analyze the thermal decay in the one-dimensional (1D) TTG experiment that corresponds to the case of a surface heating of an opaque thick SC crystal film, by solving the transient BPTE using Callaway's approximation of the collision operator. This will allow us to address and highlight more respectfully and simply the critical role of phonon-phonon scattering Normal processes. The analysis will show how considering these processes separately affects the expression of the SSF of the in-plane effective apparent thermal conductivity and the onset of the nondiffusive (quasiballistic) regime in the phonon transport process. This latter effect cannot readily be inferred from rigorous treatment using the full linearized collision matrix [16,17]. In addition, the analysis will also allow us to examine the important impact on the phonon MFP spectrum distribution that could be reconstructed based on the obtained thermal decay rate.

We present the main steps of theoretical modeling in Sec. II. In Sec. III, we discuss the results of this approach in application to the 1D TTG experiment by analyzing the effect of varying the ambient temperature. We summarize and establish our concluding remarks in Sec. IV.

II. THEORY

TTG spectroscopy technique is an experimental technique that is particularly sensitive to in-plane phonon transport [5–15]. In this section, we present the key elements of the method that allows deriving the full expression of the thermal decay rate that would be measured in this technique, by analyzing the case of a surface heating of an opaque thick SC crystal film that we can consider as a bulk material [13]. In contrast to previous theoretical works [11–15], we will consider phonon-phonon scattering Normal processes (N processes) and phonon-phonon scattering Umklapp processes (U processes) separately. Once the expression of the thermal decay rate is obtained, one can get straightforwardly the expression of the in-plane effective apparent thermal conductivity. The integrand of the latter contains the phonon SSF.

A. Callaway's approach of the Boltzmann-Peierls transport equation

The starting point of our modeling is the transient BPTE in the framework of the single-mode relaxation time approximation and using modified Debye-Callaway model in which both longitudinal and transverse phonon modes are included explicitly [18–26]. The SC system is assumed to have a cubic symmetry and is treated as a continuum, elastic, and isotropic medium characterized by a linear (Debye-like) phonon spectrum for each phonon branch polarization so that one considers heat transport due only to acoustic phonons and ignores any contribution from optical phonons [18–26]. Callaway's approximation of the collision operator in BPTE captures quite fairly and respectfully the peculiar effect of phonon-phonon N processes that distinguishes them from the rest of phonon scattering processes including phonon-phonon U processes. Thus, it allows a simple separation of N processes and U processes [18–21].

Despite its simplicity, Debye-Callaway model has been proven to be very robust and effective in the study and prediction of the steady-state temperature behavior of the thermal conductivity of SC crystals within the conventional local/linear nonequilibrium thermodynamics theory [18–25]. Besides, it constitutes one of the first models to be used to study the second sound phenomenon in SC and dielectric crystals [27]. We recently used the model to analyze the modulation frequency behavior of the reduced effective thermal conductivity of SC crystals that is observed in time-domain thermoreflectance (TDTR) and frequency-domain thermoreflectance (FDTR) experiments. We obtained an expression of the effective apparent thermal conductivity of the SC crystal that is characterized by a universal SSF that captures and describes the role, the weight, and the contribution of quasiballistic and nondiffusive phonons. The SSF only depends on the ratio between the spectral phonon MFP and the thermal penetration depth as defined based on the diffusive Fourier law [26]. Indeed, the thermal penetration depth constitutes the central characteristic length scale in TDTR and FDTR configurations.

We follow the same procedure as Collins *et al.* [13] and Hua and Minnich [11] to derive the expression of the thermal

decay in a TTG experiment. In addition, we will consider local thermal equilibrium throughout, which is required to define a temperature [18–27]. Surface heating of an opaque bulk SC crystal in a TTG experiment results in a one-dimensional spatially periodic temperature profile that we assume to be established along the direction $\vec{x}$. Under the single-mode relaxation time approximation, the transient Callaway form of the BPTE along the x axis can be written as the following [11–13,26]:

$$\frac{\partial U^m_{q,p}}{\partial t} + mv_p \frac{\partial U^m_{q,p}}{\partial x} = -\frac{U^m_{q,p} - U^0_{q,.p}}{\tau^C_{q,p}} + \frac{g^m_{q,p}}{\tau^C_{q,p}}, \tag{1}$$

where we have introduced the deviational spectral energy density per phonon mode (phonon wave packet) of wave vector $\boldsymbol{q}$ and polarization p as $U(x,t,m,q,p) \equiv U^m_{q,p} = \hbar\omega_p(n^m_{q,p} - n^{Eq}_{q,p})$. $n^m_{q,p}$ is the phonon distribution function at the absolute local thermal equilibrium temperature T. $U^0_{q,p} = \hbar\omega_p(n^0_{q,p} - n^{Eq}_{q,p})$ is therefore the deviational equilibrium spectral energy density per phonon mode with $n^0_{q,p}$ and $n^{Eq}_{q,p}$ denoting the equilibrium phonon Planck distribution functions, at temperatures T and T_0, respectively. T_0 represents an absolute reference temperature [11–13,26].

$(\tau^C_{q,p})^{-1} = (\tau^R_{q,p})^{-1} + (\tau^N_{q,p})^{-1}$ is the "combined" phonon scattering rate [18,19] with $\tau^R_{q,p}$ representing the single relaxation time with which all resistive phonon scattering processes (all scattering processes that change the total phonon wave vector: Umklapp, boundary, defects, imperfections) tend to return the phonon system to its thermal equilibrium state. $\tau^N_{q,p}$ is the single relaxation time due to N processes (scattering processes that do not change the total phonon wave vector). As pointed out by Callaway [18] and others [19–21], N processes tend to return the phonon system to a displaced ($drifted$) Planck distribution function, $n^{\lambda_p}_{q,p} = \{\exp[\frac{(\hbar\omega_p(q) - \boldsymbol{\lambda_p}.\boldsymbol{q})}{k_B T}] - 1\}^{-1}$. By symmetry consideration in cubic SC crystals, λ_p is a constant vector in the direction of the applied temperature disturbance, which has the dimension of a velocity times the reduced Planck constant $\hbar$. $\omega_p(q)$, v_p, and m are, respectively, the dispersion relation of the phonon in state (q, p), group velocity of a p-polarization phonon and directive cosine; cosine of the angle between the x axis and the phonon wave vector $\boldsymbol{q}$ [18–27].

By using Callaway's analysis and Debye-like phonon dispersion $\omega_p(q) = v_p q$ [18,19,26], we can easily show that the term $g^m_{q,p}$ is given by

$$g^m_{q,p} = -\beta_p \frac{\tau^C_{q,p}}{\tau^N_{q,p}} mv_p C^p_q \frac{dT}{dx}. \tag{2}$$

β_p is Callaway's parameter that has the dimension of a relaxation time [18–27] and $C^p_q = \frac{\partial U^0_{q,p}}{\partial T} = \hbar\omega_p \frac{\partial n^0_{q,p}}{\partial T}$ is the specific heat or heat capacity per phonon normal mode [24,26]. The Callaway pseudorelaxation time β_p describing the effect of N processes is calculated as in the conventional steady-state local/linear treatment, by recalling that N processes cannot change the total phonon wave vector (total crystal momentum) [18–27]. The term $g^m_{q,p}$ as given by Eq. (2) represents the spectral energy density per phonon mode associated with the phonon gas drift [18,19].

B. Application to the 1D TTG configuration

The one-dimensional spatially periodic temperature profile is of the form $\Delta T(x,t) = T(x,t) - T_0 = \widetilde{\Delta T}(t)e^{i\eta x}$, where $\eta = \frac{2\pi}{d}$ is the wave number of the thermal grating of spatial period d. Therefore, we seek a spatially periodic solution for $U^m_{q,p}$ of the form $U^m_{q,p}(x,t) = \widetilde{U^m_{q,p}}(t)e^{i\eta x}$. By noting that $\frac{dT}{dx} = \frac{d(\Delta T)}{dx}$, Eq. (1) becomes

$$\frac{d\widetilde{U^m_{q,p}}}{dt} + \gamma \widetilde{U^m_{q,p}} = \frac{C^p_q}{\tau_{\text{eff}}} \widetilde{\Delta T}, \tag{3}$$

where $\gamma = (\tau^C_{q,p})^{-1} + i\eta m v_p$ and $(\tau_{\text{eff}})^{-1} = (\tau^C_{q,p})^{-1} - i\eta \frac{\beta_p}{\tau^N_{q,p}} m v_p$.

To obtain Eq. (3), we used the fact that for small ΔT, we can write $\widetilde{U^0_{q,p}} = C^p_q \widetilde{\Delta T}$.

Eq. (3) is a simple one-variable first-order inhomogeneous ordinary differential equation for $\widetilde{U^m_{q,p}}$ that we can easily and readily solve. We get the following solution:

$$\widetilde{U^m_{q,p}}(\mathrm{t}) = \frac{C^p_q}{\tau_{\text{eff}}} \int_0^t e^{\gamma(t'-t)} \widetilde{\Delta T}(t')dt' + C^p_q \widetilde{\Delta T}(0)\mathrm{e}^{-\gamma t}. \tag{4}$$

Another relation between $\widetilde{U^m_{q,p}}(\mathrm{t})$ and $\widetilde{\Delta T}(t)$ is obtained through the energy conservation relation. The latter takes the form

$$\sum_p \int_{-1}^{1} \int_0^{q^p_D} \left[\frac{C^p_q}{\tau_{\text{eff}}} \widetilde{\Delta T}(t) - \frac{\widetilde{U^m_{q,p}}(\mathrm{t})}{\tau^C_{q,p}} \right] q^2 dq dm = 0, \tag{5}$$

where q^P_D denotes Debye's cutoff wave vector of the acoustic branch polarization p [18–27].

By considering the expression of $(\tau_{\text{eff}})^{-1}$, we can straightforwardly show that Eq. (5) leads to

$$\widetilde{\Delta T}(t) = \frac{\sum_p \int_{-1}^{1} \int_0^{q^p_D} \frac{\widetilde{U^m_{q,p}}(\mathrm{t})}{\tau^C_{q,p}} q^2 dq dm}{2\sum_p \int_0^{q^p_D} \frac{C^p_q}{\tau^C_{q,p}} q^2 dq}. \tag{6}$$

By inserting Eq. (4) into Eq. (6), we can directly extract the full expression of the normalized thermal decay $\tilde{Y}(t) = \frac{\widetilde{\Delta T}(t)}{\widetilde{\Delta T}(0)}$ as

$$\tilde{Y}(t) = \frac{1}{2\sum_p \int_0^{q^p_D} \frac{C^p_q}{\tau^C_{q,p}} q^2 dq} \sum_p \int_{-1}^{1} \int_0^{q^p_D} \left[\frac{C^p_q}{\tau^C_{q,p}\tau_{\text{eff}}} \int_0^t e^{\gamma(t'-t)} \times \tilde{Y}(t')dt' + \frac{C^p_q}{\tau^C_{q,p}} \mathrm{e}^{-\gamma t} \right] q^2 dq dm. \tag{7}$$

The exploitation of the expression of $(\tau_{\text{eff}})^{-1}$ allows us to rearrange Eq. (7) into a form that clearly highlights the effects of phonon-phonon scattering N processes and Callaway's model in comparison to the standard RTA model. $\tilde{Y}(t)$

can be written as

$$\tilde{Y}(t)=\frac{1}{2\sum_p\int_0^{q_D^p}\frac{C_q^p}{\tau_{q,p}^C}q^2dq}\sum_p\int_{-1}^{1}\int_0^{q_D^p}\left[\frac{C_q^p}{\left(\tau_{q,p}^C\right)^2}\int_0^t e^{\gamma(t'-t)}\tilde{Y}(t')dt'+\frac{C_q^p}{\tau_{q,p}^C}\mathrm{e}^{-\gamma t}\right]q^2dqdm$$
$$-\frac{i\eta}{2\sum_p\int_0^{q_D^p}\frac{C_q^p}{\tau_{q,p}^C}q^2dq}\sum_p\beta_p v_p\int_{-1}^{1}\int_0^{q_D^p}\left[m\frac{C_q^p}{\tau_{q,p}^C\tau_{q,p}^N}\int_0^t e^{\gamma(t'-t)}\tilde{Y}(t')dt'\right]q^2dqdm. \tag{8}$$

The first term in Eq. (8) is the result we obtain using the standard RTA model [11–15], while the additional second term represents the effect of separately taking phonon-phonon scattering N processes and U processes in the framework of the modified Debye-Callaway model [18–27].

We apply Laplace transform to Eq. (7) in order to isolate the expression of the normalized thermal decay $\widetilde{\tilde{Y}}(s)$ in Laplace domain. After performing simple calculations of the different integrals with respect to the directive cosine m and rearranging the different terms, we can straightforwardly obtain the following result:

$$\widetilde{\tilde{Y}}(s,\eta)=\frac{\sum_p\int_0^{q_D^p}C_q^p\psi_{q,p}(s,\eta)q^2dq}{\sum_p\int_0^{q_D^p}\frac{C_q^p}{\tau_{q,p}^C}\left\{1+\frac{\beta_p}{\tau_{q,p}^N}-\left[1+\frac{\beta_p}{\tau_{q,p}^N}\left(1+\tau_{q,p}^C s\right)\right]\psi_{q,p}(s,\eta)\right\}q^2dq}, \tag{9}$$

where the function $\psi_{q,p}(s,\eta)$ is given by

$$\psi_{q,p}(s,\eta)=\frac{1}{2\tau_{q,p}^C}\int_{-1}^{1}\frac{dm}{\gamma+s}=\frac{i}{2Kn_{q,p}^\eta}\log\left[\frac{1+Kn_{q,p}^S-iKn_{q,p}^\eta}{1+Kn_{q,p}^S+iKn_{q,p}^\eta}\right]=\frac{\arctan\left[\frac{Kn_{q,p}^\eta}{1+Kn_{q,p}^S}\right]}{Kn_{q,p}^\eta}, \tag{10}$$

where we introduce two nondimensional Knudsen numbers: a spatial one, $Kn_{q,p}^\eta=\eta v_p\tau_{q,p,}^C$ that compares the spectral phonon MFP to the thermal grating period, and a temporal one, $Kn_{q,p}^S=s\tau_{q,p}^C$, that compares the phonon combined relaxation time to the thermal decay time [11]. These two parameters specify the nature of the phonon transport regime completely in the spatiotemporal domain. In the diffusive limit, $Kn_{q,p}^\eta\ll 1$ and $Kn_{q,p}^S\ll 1$, while in the ballistic limit $Kn_{q,p}^\eta\gg 1$ and $Kn_{q,p}^S\gg 1$. In addition, we can obtain more insights into these regimes based on the full expression of the normalized thermal decay given by Eq. (7) as we shall see later.

The behavior of $\widetilde{\tilde{Y}}(s,\eta)$ is conditioned by the one of $\psi_{q,p}(s,\eta)$ depending on the phonon transport regime $\{Kn_{q,p}^S\to_{+\infty}^0;\ Kn_{q,p}^\eta\to_{+\infty}^0\}$.

The conventional Fourier form of the normalized thermal decay in the herein 1D TTG configuration under consideration is given by

$$Y_F(t,x)=e^{-\Gamma_F t}e^{i\eta x}, \tag{11}$$

where the thermal decay rate $\Gamma_F=\alpha_F\eta^2=\frac{\kappa_F}{C}\eta^2$; α_F, κ_F, and C are the thermal diffusivity, conductivity, and total specific heat, respectively.

If one notes $\tilde{Y}_F(t)=e^{-\Gamma_F t}$, we easily remark that the thermal decay rate will be given by

$$\Gamma_F^{-1}=\int_0^{+\infty}\tilde{Y}_F(t)dt=\widetilde{\tilde{Y}}_F(0). \tag{12}$$

We apply this formula to our result that is given by Eq. (9) and we set $\Gamma=\frac{\kappa_{\mathrm{TTG}}^{\mathrm{Callaway}}}{C}\eta^2$, where $\kappa_{\mathrm{TTG}}^{\mathrm{Callaway}}$ represents the effective apparent thermal conductivity that would be extracted from the measured thermal decay in the considered 1D TTG configuration. We easily obtain, after some algebra, the full expression of $\kappa_{\mathrm{TTG}}^{\mathrm{Callaway}}$ as

$$\kappa_{\mathrm{TTG}}^{\mathrm{Callaway}}(\eta)=\frac{C}{\sum_p\int_0^{q_D^p}C_q^p\chi_{q,p}q^2dq}\sum_p v_p^2\int_0^{q_D^p}C_q^p\tau_{q,p}^C$$
$$\times\left(1+\frac{\beta_p}{\tau_{q,p}^N}\right)\frac{1-\chi_{q,p}}{\left(Kn_{q,p}^\eta\right)^2}q^2dq, \tag{13}$$

where the function $\chi_{q,p}$ is given by

$$\chi_{q,p}(\eta)=\psi_{q,p}(0,\eta)=\frac{\arctan\left[Kn_{q,p}^\eta\right]}{Kn_{q,p}^\eta}. \tag{14}$$

III. RESULTS AND DISCUSSION

In the Theory section, we assumed that the Callaway pseudorelaxation time βp, describing the implicit effect of phonon-phonon scattering N processes, does not depend on space and that this approximation should preserve the essential features of thermal conduction by phonons. This means that the dependence of the phonon gas drift on space is contained in the expression of the drift velocity $\frac{\lambda_p}{\hbar}$ only through the temperature gradient $\nabla T(x)$ [19]. βp is a complicated quantity, depending on $\tau_{q,p}^N$ and $\tau_{q,p}^R$. This complication is necessary because of the behavior of N processes, which shuffle crystal momentum back and forth between phonon normal modes, and then contribute implicitly to the lattice thermal conduction (resistance) process of a given SC crystal material [18,19].

In order to have a closer look at the steady-state behavior of the effective apparent thermal conductivity $\kappa_{\mathrm{TTG}}^{\mathrm{Callaway}}$ and the thermal decay rate Γ as functions of the thermal grating

period and temperature, we consider natural silicon (Si) and $Si_{0.7}Ge_{0.3}$ alloy as two illustrative examples of single and alloy SC crystals, respectively. Indeed, the first experimental results regarding phonon MFP spectroscopy utilizing TTG technique were carried out on a silicon thin film [5–7]. In addition to three phonon-phonon anharmonic scattering U- and N processes, we assume scattering of phonons by the boundaries of the thick opaque SC crystal film and by impurities (defects). All geometrical and physical properties of Si and $Si_{0.7}Ge_{0.3}$ materials can be found in Tables I and II of Ref. [24]. We address particular attention to the case of Si, for which we use two different sets of expressions for the relaxation times of phonon-phonon scattering U- and N processes depending on the temperature regime. In the low-temperature regime, up to 100 K, the expressions of the relaxation times of the different phonon scattering processes considered are the conventionally and widespread ones we used in our early works [23,24]. In the high-temperature regime (>100 K), we exploit the expressions suggested by Ward and Broido based on an *ab initio* approach using first-principles density-functional perturbation theory (DFPT) [28,29]. For the case of $Si_{0.7}Ge_{0.3}$ and because of the lack of finding expressions of the relaxation times of phonon-phonon scattering U- and N processes using first-principles DFPT calculations, we assume the conventional expressions to be valid over the entire temperature range considered [23,24].

We assume all physical properties of these SC crystals to be independent of temperature. The total resistive phonon scattering rate $(\tau^R_{q,p})^{-1}$ is obtained via Matthiessen's rule [22–24].

To simplify more the expression of $\kappa^{\text{Callaway}}_{\text{TTG}}$ in Eq. (13), we express it, as it is customary in the modified Debye-Callaway model, using a sum over one longitudinal ($\kappa^{\text{Callaway}-\text{L}}_{\text{TTG}}$) and two degenerate transverse ($\kappa^{\text{Callaway}-\text{T}}_{\text{TTG}}$) phonon acoustic branch polarizations [22–26]. We also make use of the usual change of variable $y = \frac{\hbar\omega}{k_B T}$, which allows us to obtain straightforwardly the final computational expression of $\kappa^{\text{Callaway}}_{\text{TTG}}$.

A. Callaway's model vs standard RTA model

The reason that motivates the use of Callaway's model within the framework of the single-mode relaxation time approximation is the ability of this model to treat more fairly the different phonon-phonon scattering processes than does the standard RTA model. This model captures quite respectfully the peculiar effect of phonon-phonon scattering N processes that distinguishes them from the rest of the phonon scattering processes including phonon-phonon scattering U processes [18–27]. The standard RTA model, often used, does not take this difference into consideration, and it treats all phonon scattering processes similarly, as if they were all independent resistive processes. It is well known, however, that phonon-phonon scattering N processes alone do not provide thermal resistance [18,19,30].

Whether N processes are included or not in the Matthiessen rule to compute the total relaxation time in the standard RTA model has a huge impact on the final result of the steady-state behavior of the thermal conductivity κ as a function of temperature, of a bulk SC crystal. The influence is striking in the high-temperature regime above the peak value of κ as one can see in Figs. 1(a) and 1(b), in which one illustrates a very instructive comparison between Callaway's model and the standard RTA model. Figure 1 reports the computed temperature steady-state behaviors of κ of Si and $Si_{0.7}Ge_{0.3}$ using both Callaway's model and the standard RTA model with and without phonon-phonon scattering N processes included. In the low-temperature regime (below the peak value of κ), the results of the three models are undistinguishable due to boundary effects. Indeed, κ mirrors the temperature behavior of the specific heat in the low-temperature regime as boundaries phonon scattering processes dominate all other phonon scattering processes in this regime [18,19,30]. On the contrary, the three models predict different results in the high-temperature regime. The standard RTA excluding (including) N processes over (under)-estimates the value of κ in comparison to Callaway's model predictions, which fit quite fairly and consistently the experimental results [21,23]. Previous studies on Si have shown the standard RTA model including N processes to work quite well in the high-temperature regime in comparison to *ab initio* results, and the difference between this model and Callaway's to be less than few percent at 300 K [29]. As one can see in Fig. 1(a), we do not reach the same conclusion using the conventional expressions of the relaxation times of phonon-phonon scattering U- and N processes. The standard RTA model including N processes falls faster starting temperatures around 100 K and it predicts a dramatic decrease of κ of Si by almost an order of magnitude at 300 K compared to experimental values and Callaway's model. This anomaly is corrected using first-principles DFPT-based expressions of the relaxation times as illustrated in Fig. 1(b). In this figure, we used two different couples of values for Debye temperatures of the longitudinal and transverse acoustic polarization branches: (1) $\theta^L_D = 586$ K and $\theta^T_D = 240$ K; (2) $\theta^L_D = 919$ K and $\theta^T_D = 638$ K [23]. The first couple of values that correspond to the Brillouin-zone boundary frequencies are the ones we used to compute the behaviors of κ in Fig. 1(a), while the second couple of values are the ones calculated from the acoustic branch phonon velocity [23,24]. The second couple of values of Debye temperatures might be an overestimation. Nevertheless, they could be justified if one considers the contribution of optic phonon modes in the high-temperature regime. Besides, as mentioned by Ward and Broido, the first-principles DFPT-based expressions of the relaxation times of phonon-phonon scattering U- and N processes take into account the contribution to scattering events and therefore to heat transport of all phonon modes, acoustic and optic. They include also the effect of the full dispersive and anisotropic phonon branches [29]. Hence, it makes total sense that exploitation of these expressions combined with higher values of θ^L_D and θ^T_D gives better results for both Callaway's model and the standard RTA model including N processes as shown in Fig. 1(b). The two models give almost identical values over the whole temperature range that in addition fit remarkably the experimental results of natural Si. Yet, the prediction of the standard RTA model including N processes remains always below the one of Callaway's model. On the other hand, removal of such phonon-phonon scattering processes in the standard RTA model leads to a huge increase of κ. κ of Si increases by a factor of 7 at 300 K as one can

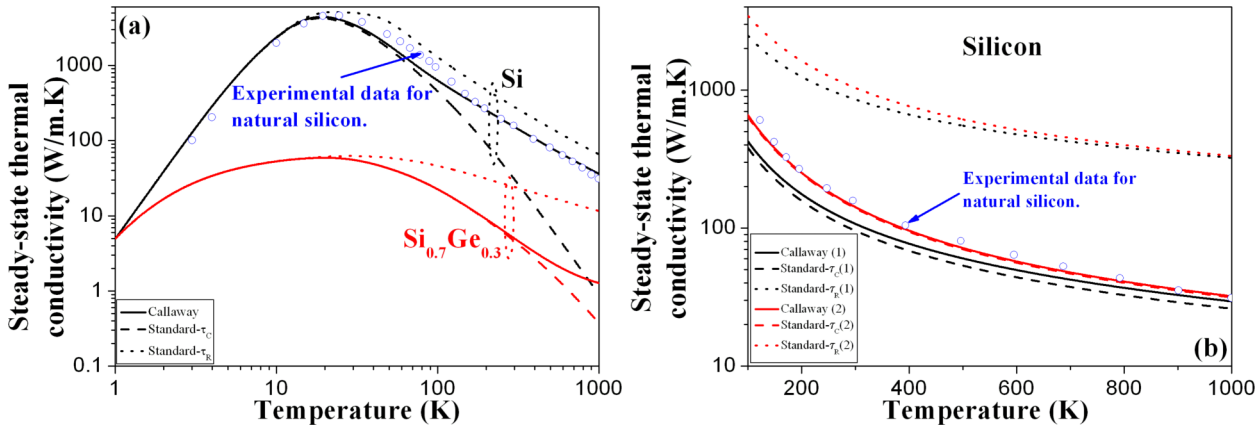

FIG. 1. (a) Computed steady-state behaviors of the thermal conductivity of Si single and $Si_{0.7}Ge_{0.3}$ alloy SC bulk crystals using the conventional expressions of the relaxation times of phonon-phonon scattering U- and N processes, as functions of temperature. Callaway's model (solid line); the standard RTA model excluding N processes (dotted line) and including them (dashed line). (b) The case of the high-temperature regime for Si using first-principles DFPT-based expressions of the relaxation times of phonon-phonon scattering U- and N processes. The experimental data of natural Si are extracted from Ref. [23].

see in Fig. 1(b). This factor remains almost the same over the whole temperature range considered, which proves the importance of phonon-phonon scattering N processes in the high-temperature regime.

The striking discrepancy in the high-temperature regime between the standard RTA model including N processes and Callaway's model, when use is made of the conventional and widespread expressions of the relaxation times of phonon-phonon scattering U- and N processes, constitutes an important and crucial point. It undoubtedly demonstrates the great sensitivity of the solution of the BPTE within the framework of the single-mode relaxation time approximation, not only to the different phonon properties and input parameters, but also and more importantly, to the particular expressions of the different relaxation times depending on the nature of the SC crystal and the temperature range. As discussed by Ward and Broido, most of the conventionally and widespread expressions of the relaxation times of phonon-phonon scattering U- and N processes were originally derived using approaches that implicitly assumed low-frequency phonons and low-temperature regime [19,30]. Thus, it is not surprising that these expressions sometimes fail to predict the correct result, especially in the high-temperature regime, depending on the used scattering term in the BPTE: standard or Callaway's and the nature of the SC crystal [29].

Furthermore, it is interesting to note that Callaway's model yields almost the same prediction of the temperature steady-state behavior of κ of Si using the two different sets of expressions for the relaxation times of phonon-phonon scattering U- and N processes.

In the case of $Si_{0.7}Ge_{0.3}$, the deviation between Callaway's model and the standard RTA model including N processes occurs starting at room temperature. Therefore, we could infer that use of the conventional expressions of the relaxation times of phonon-phonon scattering U- and N processes for this alloy SC crystal is potentially valid up to at least this temperature.

In regard to the above discussion, one could assert that a better analysis, interpretation, and exploitation of the results of the TTG technique shall arguably consider Callaway's model.

B. Phonon transport process in the 1D TTG configuration

TDTR/FDTR and TTG are two different but complementary experimental techniques that have different excitation and detection procedures. The former one is more sensitive to the cross-plane phonon transport process while the latter is more sensitive to the in-plane one. The thermal penetration depth as defined based on the diffusive Fourier law constitutes the characteristic length scale in TDTR/FDTR experiment [26]. On the other hand, and because of the nature of TTG experimental excitation and detection, no Fourier-based thermal penetration appears in the calculation, but instead the optical penetration depth could have an effect as mentioned by Chiloyan *et al.* [14] and Hubermann *et al.* [15]. In the 1D TTG configuration we are assuming in the herein work, the only characteristic length scale to be considered is the period of the thermal grating generated as a result of the interference pattern of the two crossed laser pulses shone on the surface of the opaque thick SC crystal film.

In our recent work regarding the analysis of the modulation frequency behavior of the reduced effective thermal conductivity of SC crystals that is observed in TDTR and FDTR experiments, we derived an expression of the effective apparent thermal conductivity of the SC crystal that is characterized with a universal SSF. We obtained the same SSF either using Callaway's model or the standard RTA model. In Callaway's model, we have an effective relaxation time $\tau_{q,p}^{\text{eff}} = \tau_{q,p}^{C}(1 + \frac{\beta_p}{\tau_{q,p}^{N}})$ in the integrand of the effective apparent thermal conductivity, while in the standard RTA model we have only the combined relaxation time $\tau_{q,p}^{C}$. The universality of the SSF we found was obtained naturally as a function of the only ratio of the spectral phonon MFP to the thermal penetration depth as defined based on the diffusive Fourier law. The thermal penetration depth constitutes the characteristic length scale in the TDTR/FDTR geometry once an analogy with Fourier's based thermal conductivity is sought [26].

It is interesting to note from Eq. (13) that the expression we derived for the effective apparent thermal conductivity $\kappa_{\mathrm{TTG}}^{\mathrm{Callaway}}$ that would be extracted from the measured thermal decay in the considered 1D TTG configuration has the same nonuniversal SSF that Chiloyan *et al.* found using the standard RTA model [12]. The only difference is that we have an effective relaxation time $\tau_{q,p}^{\mathrm{eff}} = \tau_{q,p}^{C}(1 + \frac{\beta_p}{\tau_{q,p}^{N}})$ that is characteristic of Callaway's model in place of just the combined relaxation time $\tau_{q,p}^{C}$ of the standard RTA. The full expression of the SSF is given by

$$\Xi_{q,p}^{\mathrm{TTG}}(\eta) = \frac{6\pi^2 C}{\sum_p \int_0^{q_D^p} C_q^p \chi_{q,p} q^2 dq} \left[\frac{1 - \chi_{q,p}}{\left(Kn_{q,p}^{\eta}\right)^2} \right]. \tag{15}$$

Hua and Minnich found the same universal SSF of Maznev *et al.* [10] due to a further assumption they used in their mathematical derivation in what they called "weak quasi-ballistic" regime [11]. If we do not use this additional assumption, the general result we obtain is a nonuniversal SSF. Hence, the nonuniversal character of the SSF of the effective apparent thermal conductivity in the 1D TTG configuration is not related to the form of the scattering term in the BPTE: standard or Callaway's. That means that considering the peculiar effect of phonon-phonon scattering N processes through Callaway's model does not influence the expression of the SSF. The latter originates from the time integration of the thermal decay that embodies time nonlocal effects as shown in Eq. (7). The appearance of time nonlocal effects is a direct consequence of solving the time-dependent BPTE in association with the initial boundary condition. These effects will indeed appear either using the standard RTA model or the full Callaway model.

Before we tackle the general spectral result of $\kappa_{\mathrm{TTG}}^{\mathrm{Callaway}}$ given by Eq. (13) and the corresponding result of the thermal decay rate, it is very instructive to discuss first the simple, yet very meaningful, case of the gray spectrum approximation (GSA). In this approximation, all phonon modes belonging to an acoustic branch polarization p have the same relaxation time independent of the wave vector q for each phonon scattering process. We shall however continue to assume separately phonon-phonon scattering N processes characterized by a relaxation time τ^N and phonon-phonon scattering resistive processes characterized by a relaxation time τ^R. In this case, we can easily show that the Callaway pseudorelaxation time β will exactly be given by τ^R. This shows the very fundamental intertwining between anharmonic N processes and resistive processes; the implicit effect of N processes in the onset of a noninfinite thermal conductivity is taken into account through the resisting causing collisions, namely the relaxation time of the resistive processes, the effect of which is explicit [24]. In addition, we assume there is no distinction between the different acoustic phonon polarizations. These assumptions shall not significantly hamper the physical picture.

Starting from the general expression of the normalized thermal decay in Laplace domain as given by Eq. (9) and applying the above assumptions, one gets straightforwardly the following GSA formula which we express using nondimensional variables $\xi = \eta\tau^R v$, $\varpi = \tau^R s$ and $\tau = \tau^R/\tau^N$:

$$\widetilde{\widetilde{Y}}_{\mathrm{GSA}}(\varpi, \xi) = \frac{\Psi(\varpi, \xi, \tau)}{(1+\tau) - \left[(1+\tau)^2 + \tau\varpi\right]\Psi(\varpi, \xi, \tau)}$$
$$\Psi(\varpi, \xi, \tau) = \frac{\arctan\left[\frac{\xi}{1+\tau+\varpi}\right]}{\xi} \tag{16}$$

Note that ξ and ϖ are nothing else than the GSA versions of the nondimensional spatial and temporal Knudsen numbers introduced above, respectively.

We report in Fig. 2 the computed behavior of the normalized thermal decay in the 1D TTG configuration in the framework of the GSA for a bulk SC crystal as a function of the nondimensional time t/τ^R for different values of the parameters τ and ξ. For large values of the thermal grating period that correspond to small values of the nondimensional spatial Knudsen number ξ, the phonon transport regime is diffusive and the normalized thermal decay decreases with time in a Fourier-like exponential fashion. As discussed by Collins *et al.,* based on the standard RTA model [13], the full solution derived from the BPTE seems to decrease slowly compared to the conventional Fourier solution. Furthermore, and as one can see in Figs. 2(a) and 2(b), consideration of the peculiar implicit effect of phonon-phonon scattering N processes through Callaway's model tends to increase the decreasing rate of the normalized thermal decay $\widetilde{\widetilde{Y}}_{\mathrm{GSA}}$. The curve of $\widetilde{\widetilde{Y}}_{\mathrm{GSA}}$ falls faster by increasing τ. As ξ increases, the phonon transport regime transitions to a quasiballistic (nondiffusive) regime, then to a full ballistic regime for very high values of ξ where the phonon MFP becomes very large in comparison to the thermal grating period. In this regime, $\widetilde{\widetilde{Y}}_{\mathrm{GSA}}$ manifests an oscillatory behavior as a function of time that is a manifestation of the phonons traveling ballistically as explained by Collins *et al.* [13]. These oscillations are due to spatial nonlocal effects [16] and could also be viewed as a signature of the phonon hydrodynamic transport regime [17]. In this case of the 1D TTG configuration, the phonons travel at a speed determined by the ratio of the thermal grating period to the period of oscillations and would be comparable to the speed of second sound [17]. Here also, the impact of the crystal momentum shuffling effect of the phonon-phonon scattering N processes is evident as the change in τ impacts both the amplitude and the period of the oscillations. It is remarkable to note however, from Figs. 2(c) and 2(d), that the oscillations seem to die off almost at the same moment independent of the value of τ. We note that the consideration of Callaway's model in the framework of the simple GSA is able to exhibit one of the most important features that was recently highlighted using rigorous analysis based on the full linearized collision matrix [16,17].

As we mentioned above, we obtain the same expression of the SSF in the integrand of the effective apparent thermal conductivity that would be extracted from the measured thermal decay in the 1D TTG configuration using both the Callaway and standard RTA models. The nonuniversal character of this SSF is captured through the term $\frac{C}{\sum_p \int_0^{q_D^p} C_q^p \chi_{q,p} q^2 dq}$ that illustrates the dependence of this function on the material

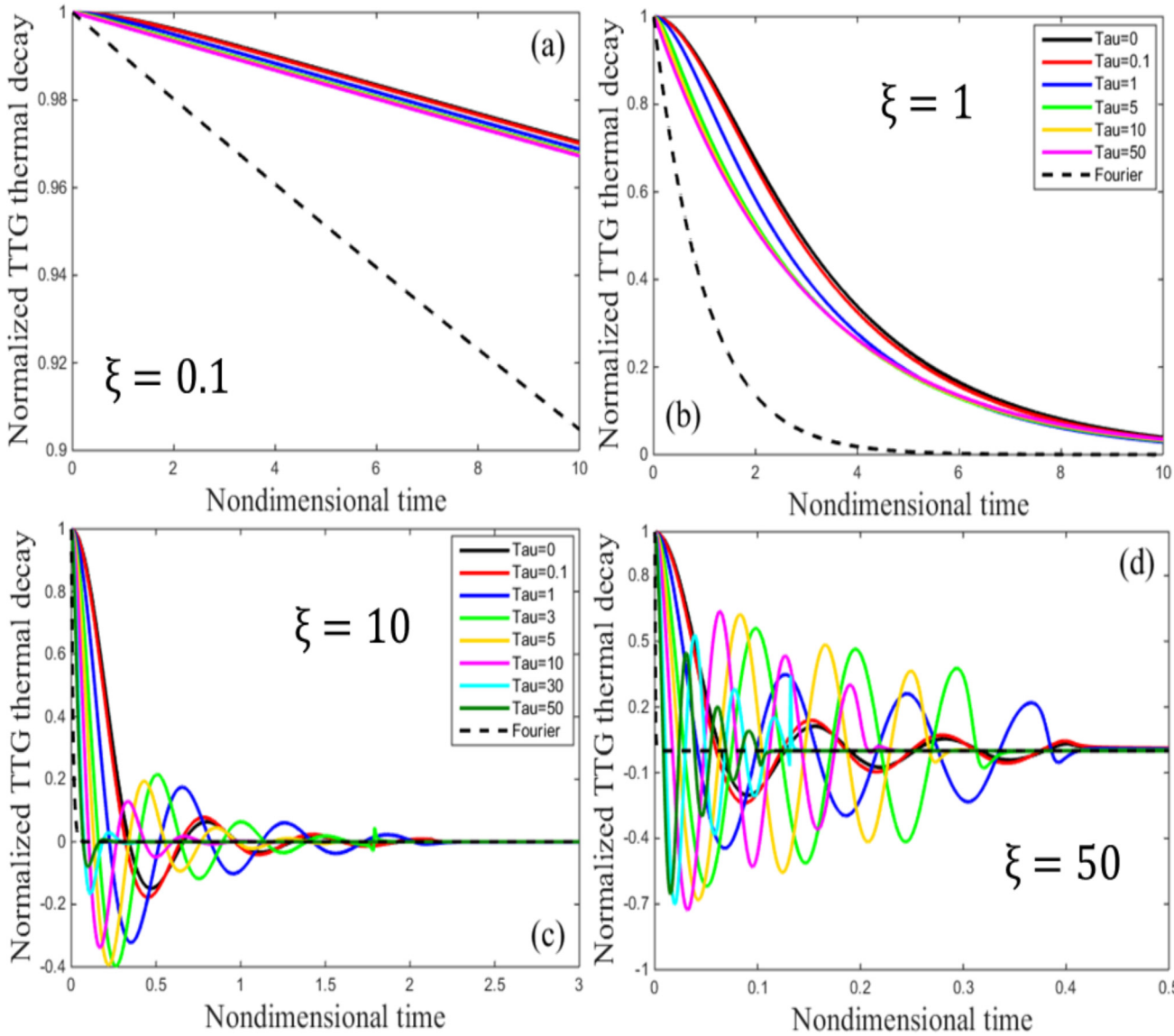

FIG. 2. Computed behavior of the normalized thermal decay in the 1D TTG configuration in the framework of the GSA for a bulk SC crystal as a function of the nondimensional time t/τ^R, for different values of the parameters τ and ξ: (a) $\xi = 0.1$, (b) $\xi = 1$, (c) $\xi = 10$, and (d) $\xi = 50$.

properties, in addition to the nondimensional spatial Knudsen number $Kn^{\eta}_{q,p}$.

In the diffusive regime ($Kn^{\eta}_{q,p} \ll 1$), $\frac{1-\chi_{q,p}}{(Kn^{\eta}_{q,p})^2}$ and $\chi_{q,p}$ tend to 1/3 and 1, respectively. Hence $\kappa^{\text{Callaway}}_{\text{TTG}}$ tends logically and naturally to the expression of steady-state Fourier thermal conductivity within the framework of the modified Debye-Callaway model [18–20,22–24]. On the other hand, in the ballistic regime limit ($Kn^{\eta}_{q,p} \gg 1$), $\frac{1-\chi_{q,p}}{(Kn^{\eta}_{q,p})^2}$ decreases as $\frac{1}{(Kn^{\eta}_{q,p})^2}$ while $\chi_{q,p}$ decreases as $\frac{1}{Kn^{\eta}_{q,p}}$; thus, $\kappa^{\text{Callaway}}_{\text{TTG}}$ will decrease as $\frac{1}{Kn^{\eta}_{q,p}}$ and ultimately tends to zero.

Figures 3(a) and 3(b) show, respectively, the computed room-temperature steady-state behaviors of the effective apparent thermal conductivity κ_{TTG} of Si and $Si_{0.7}Ge_{0.3}$ SC crystals using the conventional expressions of the relaxation times of phonon-phonon scattering U- and N processes, as functions of the thermal grating period d in the 1D TTG configuration. The figures report the results of both Callaway's model and the standard RTA model with and without N processes included. Figure 3(c) reports the case of Si using first-principles DFPT-based expressions of the relaxation times of phonon-phonon scattering U- and N processes. It is worth mentioning that for the quasiparticle description of the phonon wave packet to be valid in the first place, the minimum phonon MFP cannot be less than $2a$, where a denotes the lattice constant of the SC crystal [30]. Therefore, we set the minimum value of d to be $d_{\min} = 2a$.

For each of the three computation approaches, the behavior of κ_{TTG} shows three different regimes: (i) κ_{TTG} increases slowly as function of d for small values of the latter, then (ii) the increasing rate gets faster with d over a certain

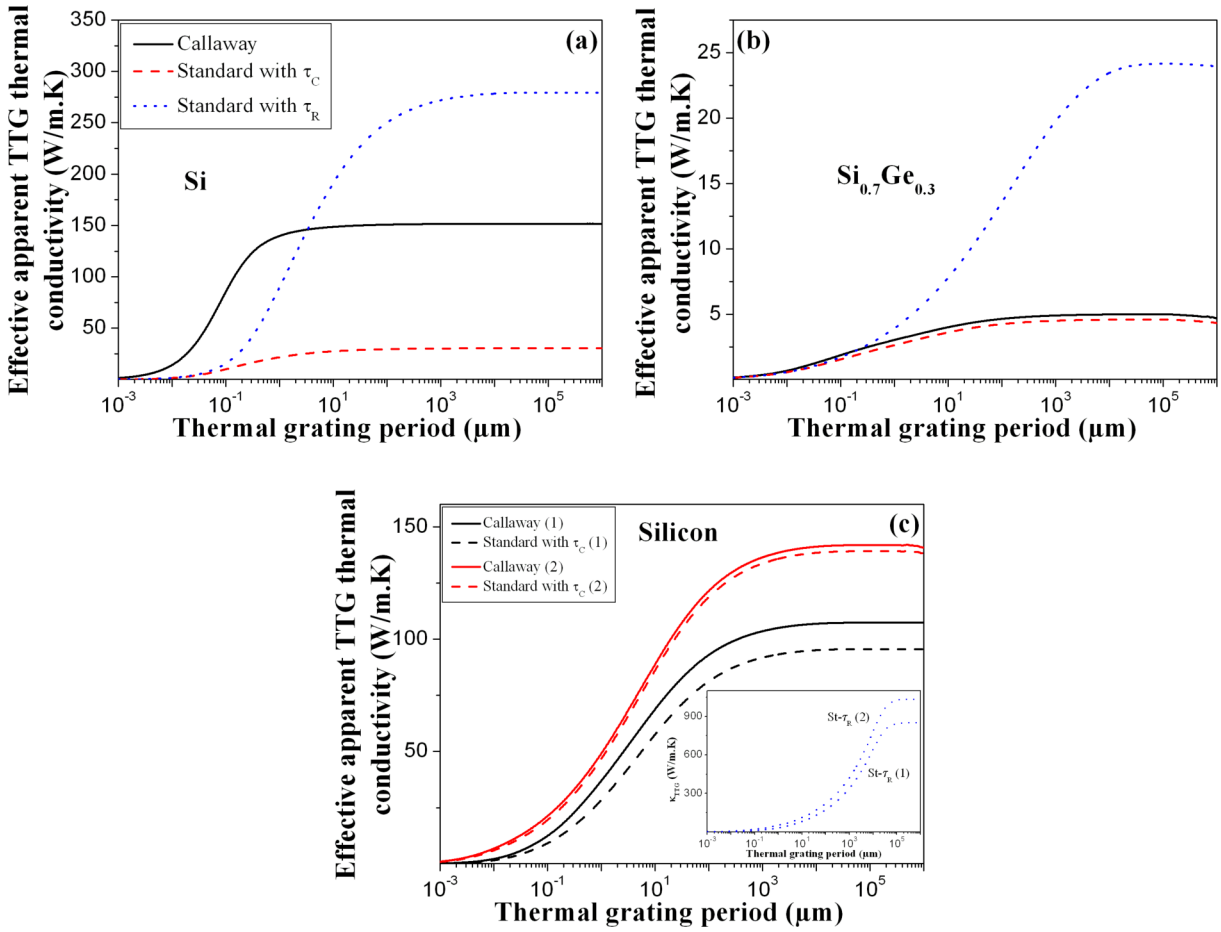

FIG. 3. Computed room-temperature steady-state behaviors of the 1D TTG effective apparent thermal conductivity of Si single (a) and $Si_{0.7}Ge_{0.3}$ alloy (b) SC bulk crystals using the conventional expressions of the relaxation times of phonon-phonon scattering U- and N processes, as functions of the thermal grating period. Callaway's model (solid line); the standard RTA model excluding N processes (dotted line) and including them (dashed line). (c) The case of Si using first-principles DFPT-based expressions of the relaxation times of phonon-phonon scattering U- and N processes.

intermediate interval, and finally (iii) κ_{TTG} saturates to a higher value for long values of d. These three regimes correspond to the quasiballistic (nondiffusive), intermediate (transitional), and diffusive ones, respectively, of the phonon transport process. Nonetheless, we clearly see in Fig. 3 how the features of these three phonon transport regimes are affected and hugely impacted by the computation model used, the nature of the SC cubic crystal: single or alloy, as well as the form of the expressions of the relaxation times of phonon-phonon scattering U- and N processes. The zone of the transition from the quasiballistic regime to the diffusive regime seems to be particularly influenced in terms of onset threshold, width, height, and increasing rate (slope). Excluding phonon-phonon scattering N processes in the standard RTA model tends to widen this quasiballistic-diffusive transition zone in addition to its dramatic overestimation of the value of κ_{TTG} in the diffusive regime. As one can see in Fig. 3(a), by using the conventional expressions of the relaxation times of phonon-phonon scattering U- and N processes, Callaway's model seems to recover the bulk thermal conductivity of Si at a shorter thermal grating period threshold (around 1 μm) than does the standard RTA model. This is an odd prediction in comparison to experimental TTG results on Si material. It is true that several published works regarding TTG experiment on Si, dealt with Si membranes or thin films [5–9]. Some samples are however thick enough to be considered as bulk materials. These works show indeed a recovery of the thermal conductivity of Si membranes starting around 7–10 μm. Once again, this anomaly is corrected using first-principles DFPT-based expressions of the relaxation times as illustrated in Fig. 3(c). Here also, we report the results using the two different couples of values for Debye temperatures of the longitudinal and transverse acoustic polarization branches. Callaway's model and the standard RTA model including N processes predict now similar behaviors where the recovery of the bulk thermal conductivity of Si starts occurring for a thermal grating period around 100 μm with a full recovery around 1000 μm. This is in total agreement with previous theoretical works in the literature that used the standard RTA model [6,12,16].

There is a small difference between Callaway's model and the standard RTA model including N processes. We will emphasize next the impact of this difference on the information we could obtain relative to the transition between the

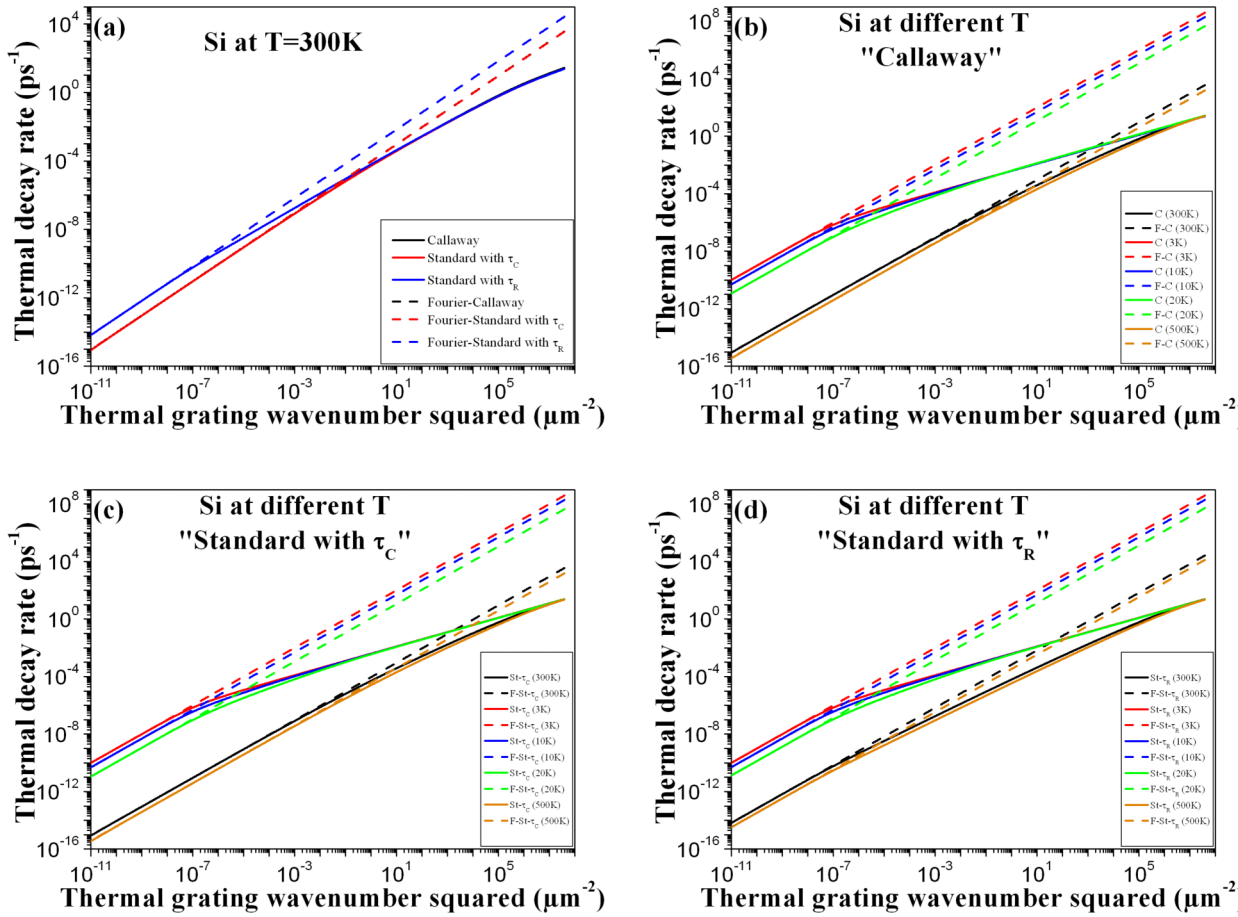

FIG. 4. Computed behaviors of the 1D TTG thermal decay rate of Si SC bulk crystal as functions of the thermal grating wave number squared using Callaway's model and the standard RTA model excluding and including phonon-phonon scattering N processes; at room temperature (a) and at different temperatures: Callaway (b), standard RTA with N processes (c), and standard RTA without N-processes (d).

diffusive and nondiffusive (quasiballistic) regimes in the phonon transport process, as well as on the phonon MFP spectrum distribution extraction in bulk SC crystals.

As mentioned by Chiloyan *et al.*, the behavior of the thermal decay rate Γ as a function of the square of thermal grating wave number η constitutes a very efficient metric that allows precise and quantitative determination of the length-scale threshold at which the phonon nondiffusive transport regime onset occurs in a TTG experiment [14]. Indeed, Γ is proportional to η^2 in the Fourier diffusive regime and the proportionality coefficient is equal to the thermal diffusivity [13,14]. Any deviation from this scaling law is an indication of a deviation of the phonon transport process from the diffusive regime.

We report, respectively, in Figs. 4 and 5, the computed behaviors of Γ in the 1D TTG configuration as functions of η^2 for Si and $Si_{0.7}Ge_{0.3}$ SC crystals at different temperatures for the three models considered: Callaway's model and the standard RTA model with and without N processes included.

We remind here that in the case of Si, we use the conventional expressions of the relaxation times of phonon-phonon scattering U- and N processes for the temperatures 3, 10, and 20 K and we use first-principles DFPT-based expressions of these relaxation times for the temperatures 300 and 500 K. In the case of $Si_{0.7}Ge_{0.3}$, we use the conventional expressions of these relaxation times for all temperatures, as we mentioned in the beginning of the Results and Discussion section.

As one can see in these figures, the three models show the deviation of the phonon transport process from the Fourier diffusive regime to occur at different thresholds depending on ambient temperature T. For each of the approaches, Γ decreases and η, at which the quasiballistic (nondiffusive) phonon transport regime starts to manifest itself, shifts to higher values by increasing T. This means that the onset length-scale threshold of the nondiffusive phonon transport regime decreases as expected by increasing T. Indeed, the phonon MFP decreases by increasing T [30]. We note also that in the ballistic limit ($Kn^{\eta}_{q,p} \to +\infty$), (i) the three approaches collapse on each other and (ii) for each approach, all the curves for different T collapse on each other as expected, in accordance with the tendencies in Figs. 3(b) and 3(c).

In the TTG configuration, the characteristic length scale of the experiment (thermal grating period) does not depend on the model: Callaway's or standard RTA. We define the length-scale threshold at which there will be a transition in the phonon transport process from the nondiffusive (quasiballistic) regime to the diffusive regime, as the thermal grating

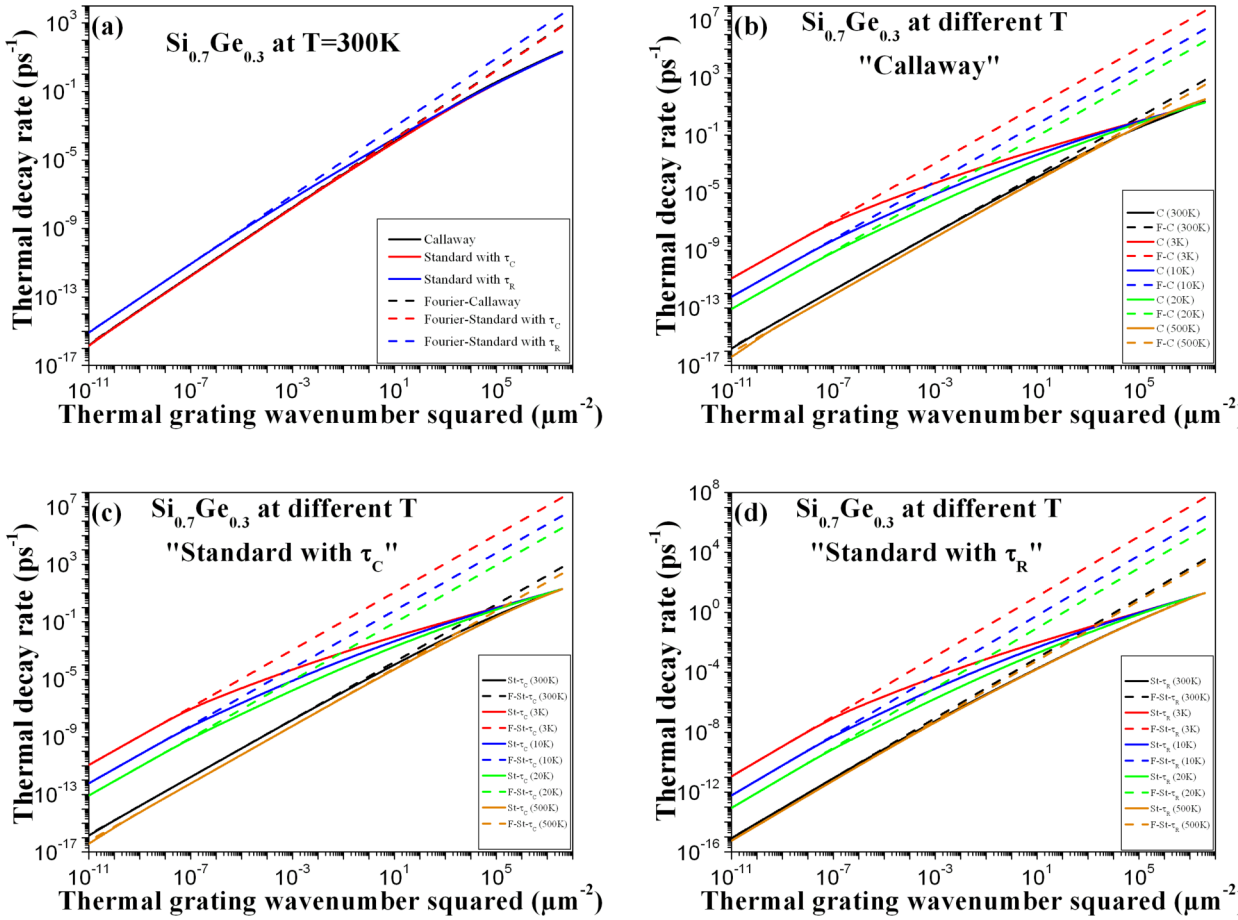

FIG. 5. Computed behaviors of the 1D TTG thermal decay rate of $Si_{0.7}Ge_{0.3}$ SC bulk crystal as functions of the thermal grating wave number squared using Callaway's model and the standard RTA model excluding and including phonon-phonon scattering N processes; at room temperature (a) and at different temperatures: Callaway (b), standard RTA with N processes (c), and standard RTA without N processes (d).

period for which $\Gamma/\Gamma_F = 0.99$. We summarize in Table I the values of these thresholds obtained from Figs. 4 and 5 for both Si and $Si_{0.7}Ge_{0.3}$ SC crystals using the three different models at different temperatures.

The length-scale threshold ranges from centimeters in the low-T regime to millimeters in the high-T regime. At each T and for each SC crystal, the behavior of the threshold for the three different models used mirrors, to a certain point, the steady-state T behavior of the thermal conductivity κ discussed above in Fig. 1. The three models lead to almost the same values of the length-scale threshold for temperatures below the optimal T_{op} of the peak value of κ and start to depart from each other for temperatures above T_{op}. For each SC crystal above its T_{op}, Callaway's model shows the lowest threshold and the standard RTA model without phonon-phonon scattering N processes included shows the highest. It is worth noticing also that both Si and $Si_{0.7}Ge_{0.3}$ manifest very close length-scale thresholds for the onset of nondiffusive phonon

TABLE I. Computed thermal grating period thresholds at which $\Gamma/\Gamma_F = 0.99$ for both Si and $Si_{0.7}Ge_{0.3}$ SC bulk crystals at different temperatures, using Callaway's model and the standard RTA model excluding and including phonon-phonon scattering N processes.

Temperature (K)	Thermal grating period threshold at 99% of Fourier's diffusive regime					
	Callaway		Standard RTA with τ_C		Standard RTA with τ_R	
	Si	$Si_{0.7}Ge_{0.3}$	Si	$Si_{0.7}Ge_{0.3}$	Si (cm)	$Si_{0.7}Ge_{0.3}$ (cm)
3	15.783 cm	13.126 cm	15.783 cm	13.126 cm	15.783	13.126
10	14.393 cm	10.667 cm	14.393 cm	10.667 cm	14.729	10.915
20	9.727 cm	9.289 cm	9.954 cm	9.289 cm	11.97	9.954
300	5.581 mm	2.324 mm	5.712 mm	2.608 mm	9.506	2.277
500	3.52 mm	226.649 μm	3.602 mm	403.279 μm	9.506	1.403

TABLE II. Computed thermal grating period thresholds at which $\Gamma/\Gamma_F = 0.99$ for Si SC bulk crystal in the high-temperature regime, using Callaway's model and the standard RTA model including phonon-phonon scattering N processes.

	Thermal grating period threshold at 99% of Fourier's diffusive regime (mm)		
	Callaway	Standard RTA with τ_C	Relative difference (%)
Temperature (K)	d_C	d_{τ_C}	$(d_{\tau_C} - d_C)/d_{\tau_C}$
100	15.747	16.114	2.28
200	8.07	8.259	2.29
300	5.581	5.712	2.29
500	3.52	3.602	2.28
800	2.434	2.491	2.29

transport regime for temperatures in the vicinity of their T_{op}, which happen to be around 20 K for both SC crystals as can be seen in Fig. 1. We could attribute this result to the fact that in the neighboring κ peak, all phonon scattering processes, intrinsic and extrinsic, are important and all contribute significantly [28]. Since κ of both Si and $Si_{0.7}Ge_{0.3}$ reaches its peak value at almost the same T_{op}, this means that the interplay mechanism between the different phonon scattering processes in the vicinity of this temperature would have comparable strengths or magnitudes in both SC crystals.

In order to shed more light on the implications of the difference between Callaway's model and the standard RTA model including N processes, we report in Table II the values of the thermal grating period threshold defined in Table I in the case of Si in the high-temperature regime.

The relative difference between the values of the thermal grating period thresholds obtained using the two approaches remains almost the same over the whole high-temperature range and is equal to ∼2.3%. It is remarkable to notice that this is very close to the relative difference between the values of the steady-state thermal conductivities κ obtained using these approaches $(\kappa_{\text{Callaway}} - \kappa_{\text{RTA}-\tau_C})/\kappa_{\text{Callaway}}$. Nevertheless, while in the study of the temperature behavior of the steady-state κ this difference might be considered negligible, this cannot be the case when investigating the phonon MFP spectrum distribution. This fact consolidates and highlights the importance of Callaway's model.

It is interesting to remind that in our 1D TTG experiment configuration for an opaque thick film (bulk material) SC crystal, there is no scattering process of phonons associated with the thermal grating period; the thermal grating does not physically reduce the phonon MFP [13]. The boundary scattering process we assumed in our computations corresponds to a fixed effective length scale that is representative of a bulk material [24].

In order to have an approximative yet very instructive physical picture of the effect of phonon-phonon scattering N processes in the framework of Callaway's model on the onset of the nondiffusive phonon transport regime, we could use the simple argument of the GSA approach as we did above. In light of this approach and based on a combination of Eqs. (12) and (16), one could straightforwardly get

$$\tau^R\Gamma(\tau,\xi) = (1+\tau)\frac{\xi - (1+\tau)\arctan\left[\frac{\xi}{1+\tau}\right]}{\arctan\left[\frac{\xi}{1+\tau}\right]}. \tag{17}$$

Moreover, we can easily show that $\tau^R\Gamma_F = \xi^2$ in this case. One sets the real number $0 < n < 1$ such that $\Gamma/\Gamma_F = n$. Thus, one could show, after some algebra, that we obtain the following equation:

$$\arctan(Z) = \frac{Z}{1+nZ^2}$$
$$Z = \frac{\xi}{1+\tau}. \tag{18}$$

If Z_n is the solution of Eq. (18), then one could write

$$\xi_n = Z_n\tau + Z_n = \frac{2\pi\tau^R v}{d_n}. \tag{19}$$

The length-scale threshold d_n for the onset of the nondiffusive phonon transport regime at $100n\%$ of the Fourier diffusive regime scales, therefore, inversely to $\tau = \tau^R/\tau^N$. The peculiar crystal momentum shuffling effect of phonon-phonon scattering N processes tends thus, independently from the other phonon scattering processes, to reduce the length-scale threshold of occurrence of the transition from the diffusive regime to the nondiffusive (quasiballistic) regime in the phonon transport process. Consequently, it favors the maintenance of the phonon diffusive regime over a large length-scale range. The standard RTA model excluding phonon-phonon scattering N processes is unable to unveil this remarkable feature, which nonetheless will be hidden when using the standard RTA model including these processes. Callaway's model sheds light on this key characteristic of N processes straightforwardly. This simple analysis using the GSA approach confirms very well the results of the general spectral case shown in Tables I and II above.

Phonon-Phonon scattering N processes are treated similarly to all other phonon scattering processes in the standard RTA model [30]. This does not mean they are not considered important. But rather, we commonly neglect in such a model the particularity these scattering processes have of shuffling the crystal momentum between the different phonon normal modes [18,19,30]. The use of Callaway's model captures this peculiar effect twice: first, through the combined relaxation time and second, through Callaway's parameter, which leads to an additional term to the standard RTA model [18,19]. Therefore, by using the standard RTA model, we miss this effect either by including or excluding phonon-phonon scattering N processes in the total relaxation time. This can be justified in the steady-state low temperature regime but

not in the steady-state high-temperature regime, where consideration of the peculiar implicit effect of phonon-phonon scattering N processes becomes more relevant.

All the above results we obtained in the framework of Callaway's approach of the collision operator in the BPTE shed light on the fundamental role of phonon-phonon scattering N processes in the intrinsic intertwining interaction between low- and high-frequency phonons that leads to the onset of the nondiffusive (quasiballistic)-diffusive transition regime in the phonon transport process in cubic SC crystals in the 1D TTG configuration. As such, the approach would allow obtaining more details and information about this intermediate regime than what we can get based on the standard RTA approach used in previous works [5–15]. The accumulation function and, more precisely, the thermal conductivity per phonon MFP are directly influenced.

Furthermore, the contribution weights of phonons with MFP within this quasiballistic-diffusive transition regime can be very sensitive to temperature, the SC crystal thin-film thickness, as well as the depth of the dissipated heat inside the latter. The study of the 1D TTG configuration we performed in the present work can be deepened and enlarged to a multidimensional TTG configuration, in order to evaluate the real impact of Callaway's model in phonon spectroscopy. Indeed, the SSF in the framework of this model will be important for a more accurate prediction of thermal conductivity reduction over the entire phonon spectrum. This will allow a better understanding of how thermal length scales in the TTG experiment affect which phonons conduct heat in each transport regime, in a rather simpler manner. To a certain point, this will be equivalent to the rigorous treatment based on the full linearized collision matrix used in recent works [16,17]. Of course, these works have the merit of a more accurate physical picture. But, Callaway's model big advantage and great usefulness will lie in its simplicity and reduced computational cost with the aim of applying a reconstruction method to obtain the phonon MFP spectral distribution from the experimentally measured thermal decay in the TTG experiment [5,31,32]. The method used in the case of the standard RTA model will have to be modified [5]. This would probably increase the sensitivity of the reconstruction method to hyperparameters [33], but this is beyond the scope of the present work.

IV. CONCLUSIONS

An approach based on solving the transient single-mode relaxation time approximated Boltzmann-Peierls transport equation in the framework of modified Debye-Callaway model has been developed to analyze the thermal decay of opaque thick semiconductor cubic crystal films in the 1D configuration of the transient thermal grating experiment. We have obtained a nonuniversal spectral suppression function in the integrand of the effective apparent thermal conductivity that is similar to the one obtained using the standard single-mode relaxation time approximation model. The only difference is that we have an effective relaxation time $\tau_{q,p}^{\text{eff}} = \tau_{q,p}^{C}(1 + \frac{\beta_p}{\tau_{q,p}^{N}})$ that is characteristic of Callaway's model in place of just the combined relaxation time $\tau_{q,p}^{C}$ of the standard RTA model. This proves that the nonuniversal character of the SSF in the TTG experiment does not depend on the form of the collision operator approximation in the BPTE: Callaway's or standard. The SSF captures and describes very well the intertwining interaction between low- and high-frequency phonons in the onset of the quasiballistic (nondiffusive) heat transport regime and as such, the reduction of the effective apparent thermal conductivity of SC crystals observed in TTG experiments.

Callaway's approach unveils the central and relevant role that the meticulously implicit shuffling effect of the crystal momentum by phonon-phonon scattering N processes plays in the onset of the nondiffusive (quasiballistic) regime in the phonon transport process in SC crystals. Thus, the peculiar effect of phonon-phonon scattering N processes captured by Callaway's model has undoubtedly an impact on the extraction of the phonon MFP spectrum distribution, especially in the high-temperature regime.

[1] D. G. Cahill, W. K. Ford, K. E. Goodson, G. D. Mahan, A. Majumdar, H. J. Maris, R. Merlin, and S. R. Phillpot, J. Appl. Phys. **93**, 793 (2003).

[2] D. G. Cahill, P. V. Braun, G. Chen, D. R. Clarke, S. Fan, K. E. Goodson, P. Keblinski, W. P. King, G. D. Mahan, A. Majumdar, H. J. Maris, S. R. Phillpot, E. Pop, and L. Shi, Appl. Phys. Rev. **1**, 011305 (2014).

[3] A. Henry and G. Chen, J. Comput. Theor. Nanosci. **5**, 141 (2008).

[4] L. Lindsay, D. A. Broido, and T. L. Reinecke, Phys. Rev. B **87**, 165201 (2013).

[5] A. J. Minnich, Phys. Rev. Lett. **109**, 205901 (2012).

[6] J. A. Johnson, A. A. Maznev, J. Cuffe, J. K. Eliason, A. J. Minnich, T. Kehoe, C. M. Sotomayor Torres, G. Chen, and K. A. Nelson, Phys. Rev. Lett. **110**, 025901 (2013).

[7] J. Cuffe, J. K. Eliason, A. A. Maznev, K. C. Collins, J. A. Johnson, A. Shchepetov, M. Prunnila, J. Ahopelto, C. M. Sotomayor Torres, G. Chen, and K. A. Nelson, Phys. Rev. B **91**, 245423 (2015).

[8] J. A. Johnson, J. K. Eliason, A. A. Maznev, T. Luo, and K. A. Nelson, J. Appl. Phys. **118**, 155104 (2015).

[9] A. Vega-Flick, R. A. Duncan, J. K. Eliason, J. Cuffe, J. A. Johnson, J.-P. M. Peraud, L. Zeng, Z. Lu, A. A. Maznev, E. N. Wang, J. J. Alvarado-Gil, M. Sledzinska, C. M. Sotomayor Torres, G. Chen, and K. A. Nelson, AIP Adv. **6**, 121903 (2016).

[10] A. A. Maznev, J. A. Johnson, and K. A. Nelson, Phys. Rev. B **84**, 195206 (2011).

[11] C. Hua and A. J. Minnich, Phys. Rev. B **89**, 094302 (2014).

[12] V. Chiloyan, L. Zeng, S. Huberman, A. A. Maznev, K. A. Nelson, and G. Chen, Phys. Rev. B **93**, 155201 (2016).

[13] K. C. Collins, A. A. Maznev, Z. Tian, K. Esfarjani, K. A. Nelson, and G. Chen, J. Appl. Phys **114**, 104302 (2013).

[14] V. Chiloyan, L. Zeng, S. Huberman, A. A. Maznev, K. A. Nelson, and G. Chen, J. Appl. Phys. **120**, 025103 (2016).

[15] S. Huberman, V. Chiloyan, R. A. Duncan, L. Zeng, R. Jia, A.

A. Maznev, E. A. Fitzgerald, K. A. Nelson, and G. Chen, Phys. Rev. Materials **1**, 054601 (2017).
[16] C. Hua and L. Lindsay, Phys. Rev. B **102**, 104310 (2020).
[17] V. Chiloyan, S. Huberman, Z. Ding, J. Mendoza, A. A. Maznev, K. A. Nelson, and G. Chen, Phys. Rev. B **104**, 245424 (2021).
[18] J. Callaway, Phys. Rev. **113**, 1046 (1959).
[19] P. Carruthers, Rev. Mod. Phys. **33**, 92 (1961).
[20] M. G. Holland, Phys. Rev. **132**, 2461 (1963).
[21] R. E. Nettleton, Phys. Rev. **132**, 2032 (1963).
[22] M. Asen-Palmer, K. Bartkowski, E. Gmelin, M. Cardona, A. P. Zhernov, A. V.Inyushkin, A. Taldenkov, V. I. Ozhogin, K. M. Itoh, and E. E. Haller, Phys. Rev. B **56**, 9431 (1997).
[23] D. T. Morelli, J. P. Heremans, and G. A. Slack, Phys. Rev. B **66**, 195304 (2002).
[24] Y. Ezzahri and K. Joulain, J. Appl. Phys. **112**, 083515 (2012).
[25] J. Ma, W. Li, and X. Luo, Phys. Rev. B **90**, 035203 (2014).
[26] Y. Ezzahri, K. Joulain, and J. Ordonez-Miranda, J. Appl. Phys. **128**, 105104 (2020).
[27] R. A. Guyer and J. A. Krumhansl, Phys. Rev. **133**, A1411 (1964).
[28] D. A. Broido, M. Malorny, G. Birner, N. Mingo, and D. A. Stewart, Appl. Phys. Lett. **91**, 231922 (2007).
[29] A. Ward and D. A. Broido, Phys. Rev. B **81**, 085205 (2010).
[30] J. M. Ziman, *Electron and Phonons* (Oxford University Press, New York, 1960).
[31] M. Forghani, N. G. Hadjiconstantinou, and J.-P. M. Péraud, Phys. Rev. B **94**, 155439 (2016).
[32] M. Forghani and N. G. Hadjiconstantinou, Appl. Phys. Lett. **114**, 023106 (2019).
[33] M. A. Sanchez-Martinez, F. Alzina, J. Oyarzo, C. M. Sotomayor-Torres, and E. Chavez-Angel, Nanomaterials **9**, 414 (2019).